Compositional Space Parameterization: Theoretical Background and Application for Immiscible Displacement

D.V. Voskov, SPE, Stanford U. and **H.A. Tchelepi**, SPE, Stanford U.;

Summary

Thermodynamic equilibrium (flash) calculations in compositional flow simulators are used to find the partitioning of components among fluid phases. The nonlinear thermodynamic equilibrium relations for each gridblock are solved separately from the hydrodynamic flow equations. This step can be a time consuming kernel in a compositional flow simulation. We describe a tie-line based compositional space parametrization approach for dealing with immiscible gas injection displacement processes involving large numbers of components. The multi-component multi-phase equilibrium problem can be recast in terms of this parameterized compositional space, in which the solution path of is represented in natural manner.

We use this space parametrization approach to speed up the phase behavior calculations of standard compositional simulation. The flash calculations are performed in a preprocessing stage and the results are stored in a table. During the course of a simulation, the flash calculation procedure is replaced by the solution of an optimization for a multi-dimensional equilibrium problem in terms of the parameterized space. For processes where significant changes in pressure and temperature take place, this optimization procedure is combined with linear interpolation in tie-line space. We demonstrate our approach using one-dimensional numerical examples of multi-component immiscible gas injection.

Adaptive compositional space parametrization is used to speed up the standard phase split calculation of standard approaches. In gas injection processes, the displacement path in compositional space takes place along a limited number of tie-lines. This fact is used to avoid redundant stability checks. Specifically, given a composition, we check if it belongs to one of tie-lines, or its extension, already in the table. If not, a new tie-line is computed and added to the table. This Compositional Space Adaptive Tabulation (CSAT) technique was implemented in a general-purpose research simulator (GPRS), which is designed for compositional flow modeling on unstructured grids. Using a variety of challenging models, we show that for immiscible compositional processes, CSAT leads to significant speed up (at least a several-fold improvement) of the flash calculations compared to standard techniques.

Introduction

Gas injection processes for enhanced oil recovery are described using compositional models that account for the transfer of components between multiple fluid phases. Compositional reservoir simulators usually employ an Equation of State (EOS) model to describe the phase behavior Coats (1980) - Aziz and Wong (1988). For each computational cell (control volume) in the reservoir model, given temperature, pressure, and the overall composition of each component in the mixture, EOS computations are used to determine the phase state (liquid, vapor, or both) and the phase compositions at thermodynamic equilibrium. These EOS calculations are time consuming, and several challenges remain.

The computational cost of compositional flow simulation increases dramatically with the number of components used to represent the fluid system. As a result, it is common practice to use a lumping procedure to represent the thermodynamic behavior using a small set of pseudo components. There have been several attempts to describe gas injection recovery processes using a pseudo-ternary representation Helfferich (1981)−Tang and Zick (1993). Many investigators proposed that such ternary representations may in fact be applicable for general multi-component problems.

In the 1990's, Orr and coworkers including Monroe et al. (1990), Johns et al. (1993a), Johns et al. (1993b) studied gas injection processes for oil recovery. They presented a unified Method of Characteristics (MOC) theory of multi-contact miscible one-dimensional gas-injection processes for mixtures with large numbers of components. Orr and coworkers showed that the structure and properties of the tie-lines dictate the solution route in compositional space. We now know that displacements involving more than three components display significantly different flow behaviors from those associated with pseudo-ternary models. Based on the ideas of Monroe et al. (1990) - Orr (2007), an alternative approach to compositional modeling was developed Entov (1997) - Voskov et al. (2001). In this approach, the description of gas injection processes is simplified using a parametrization of the compositional space based on tie-lines. A similar approach was suggested by Bedrikovetsky and Chumak (1992). for systems with constant-partitioning coefficients.

Significant progress has been made over the last decade in improving the robustness and efficiency of standard EOS-based phase behavior computations. For example, there is the way to improve the speed of standard flash computations for miscible gas displacement Michelsen (1998). Several advance methods for phase stability computations was developed as well. Firoozabadi and Pan (2002) describe a reduced variable method to improve the robustness and efficiency of the phase behavior calculations. Another possibility is to use some heuristics in order to reduce the number of routine stability checks during simulation (Rasmussen et al. (2006)).

The paper is organized as follows. Since our proposed method is aimed at speeding up standard EOS-based simulation, we begin with a description of the standard approach. Then, we present the compositional space parametrization (CSP) framework for dealing with multi-component immiscible displacement processes, and we discuss solution invariance in tie-line space. We then describe an adaptive tabulation strategy. The robustness and computational efficiency of the CSP based schemes are demonstrated using several challenging gas injection problems. The summary and conclusions are given in the last section.

Conventional Compositional Simulation Approach

For a mixture of n_c hydrocarbon components and two hydrocarbon phases, the mathematical statement expressing the state of thermodynamic equilibrium can be written as

$$f_{i,V}(p,T,y_i) - f_{i,L}(p,T,x_i) = 0, \quad i \in [1 \dots n_c] \dots . \quad (1)$$

$$z_i - (1-L)y_i - Lx_i = 0, \quad i \in [1 \dots n_c] \dots . \quad (2)$$

$$\sum_{i=1}^{n_c} (x_i - y_i) = 0, \dots \dots \dots \dots \dots \quad (3)$$

where p, T, and z_i denote pressure, temperature and overall mole fractions of component i, respectively; x_i and y_i represent oil and gas mole fractions; L is the mole fraction of feed in the liquid phase; $f_{i,V}(p,T,y_i)$ and $f_{i,L}(p,T,x_i)$ represent the fugacity of component i in vapor and liquid phases respectively. We assume that p, T, and

This paper (SPE 106029) was revised for publication from paper SPE 106029, presented at the 2007 SPE Reservoir Simulation Symposium held in The Woodlands, Texas, U.S.A., 26-28 February 2007. Original manuscript received for review December 14, 2006. Revised manuscript received November 15, 2007. Manuscript peer approved August 4, 2008.

z_i are known and that $f_{i,j}$ are governed by a nonlinear function, and we need to find x_i, y_i and L.

The following procedure is used to describe the phase behavior at equilibrium:

- Phase stability test: for the current p, T and z_i, find the phase state (liquid, vapor, or two-phase) of this composition. This test is needed for any cell whose status in the previous iteration was single-phase.
- Flash calculation: when the phase stability test indicates that the cell phase state changed from one to two phases, we need to solve the system (1) - (3) in order to obtain the x_i, y_i and L.

The phase stability test in modern reservoir simulators is usually performed using Michelsen (1982) approach . For the flash calculations, a combination of Successive Substitution Iteration (SSI) and Newton method is usually used (Michelsen and Mollerup (2004)).

Compositional Space Parametrization.

We present a new approach for compositional flow simulation. The method is based on tie-line parametrization of the compositional space. We describe the method, and we demonstrate its robustness and computational efficiency using comparisons with the standard EOS-based approach.

Consider a system of n_c components. The independent overall mole fraction of the i-th component, z_i, in the mixture is defined by equation (2). Using one of the components, say the first one, we can write

$$L = \frac{z_1 - y_1}{x_1 - y_1}. \qquad \ldots\ldots\ldots\ldots\ldots\ldots\ldots\ldots \quad (4)$$

We use the structure and properties of the tie-line space to parameterize the compositional space. This is possible because along a tie-line, or its extension, the overall concentration and fractional flow of a component can be written as a linear function of one component concentration (say the first) and the tie-line parameters (Orr (2007), Entov (1997)). To show this, we substitute Eq. (4) into Eq. (2), which leads to

$$z_i = A_i z_1 + B_i, \quad i = 2 \ldots n_c - 1, \qquad \ldots\ldots\ldots\ldots \quad (5)$$

where

$$A_i = \frac{x_i - y_i}{x_1 - y_1}, \quad B_i = y_i - y_1 \frac{x_i - y_i}{x_1 - y_1}. \qquad \ldots\ldots\ldots \quad (6)$$

The parameters A_i and B_i are constants for a given tie-line in the two-phase region, or its extension (see Fig.1), and they change only when we change tie-lines.

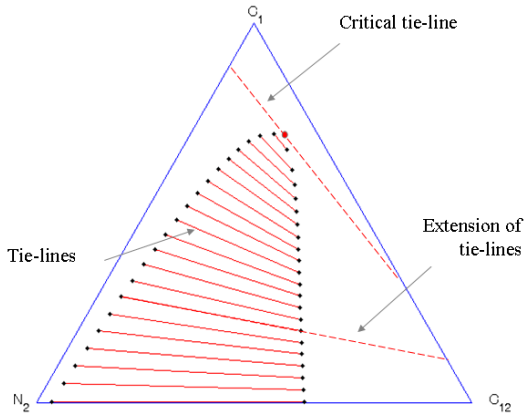

Fig. 1—Ternary diagram for $\{N_2, C_1, C_{12}\}$ at $p = 2650$ psi, $T = 480^o$ F

We replace the composition vector $\mathbf{z}, \{z_i, i = 1 \ldots n_c - 1\}$ with a new set of independent variables, namely, z_1 and $\gamma = \{\gamma_i, i = 1 \ldots n_c - 2\}$. The vector γ is constant for a particular tie-line. The quantities x_1, y_1, A_i and B_i are easily written in terms of γ. For example, under certain assumptions the thermodynamic behavior of these quantities in γ-space can be described using polynomial approximations (Voskov et al. (2001), Voskov (2002)). In practice, the compositional space can be represented reasonably well using a finite number of tie-lines.

Notice that the definition in (6) means that for cases when x_1 is close to y_1, we may have problems. This occurs when (1) we are close to the plane $z_1 \equiv 0$, or (2) when we are close to the critical region (i.e., beyond the region of tie-line extensions). In the first case, we switch to another primary component. This can be done easily based on the $\{z_i\}$ distribution. For case 2, standard EOS-based methods can be used.

Solution invariance

Parametrization of the tie-line space using the new tie-line based variable set allows us to split the overall problem of compositional reservoir flow simulation into thermodynamic and hydrodynamic parts (Entov (1997)). Consider the system of conservation laws for 1D incompressible two-phase flow in porous media

$$\phi \frac{\partial z_i}{\partial t} + U \frac{\partial F_i}{\partial x} = 0, \quad i = 1, \ldots, n_c - 1, \qquad \ldots\ldots\ldots \quad (7)$$

where F_i is the overall fractional flow of component i defined as $F_i = x_i F(s) + y_i (1 - F(s))$, and $F(s)$ is the fractional flow of the liquid phase, U is total velocity, and ϕ is porosity of reservoir. Using the tie-line based parametrization in terms of z_1 and γ, the system of equations (7) can be written as follows:

$$\phi \frac{\partial z_1}{\partial t} + U \frac{\partial F_1}{\partial x} = 0, \qquad \ldots\ldots\ldots\ldots \quad (8)$$

$$m \frac{\partial A_i z_1 + B_i}{\partial t} + U \frac{\partial A_i F_1 + B_i}{\partial x} = 0. \qquad \ldots\ldots\ldots\ldots \quad (9)$$

Here $i = 2, \ldots, n_c - 1$. To simplify the description, we take $U/\phi = 1$.

A splitting procedure is used to solve (8)-(9). First, the (auxiliary) thermodynamic problem is formulated in terms of A_i and B_i, which takes the following form

$$\frac{\partial A_i(\gamma)}{\partial t} + \frac{\partial B_i(\gamma)}{\partial y} = 0, \quad i = 2, \ldots, n_c - 1. \qquad \ldots\ldots \quad (10)$$

Here y is an auxiliary dimensional variable different from x. Notice that A_i and B_i are only functions of γ. Thus, the solution of this problem (10) depends only on the thermodynamic behavior of the system and is independent of the hydrodynamic properties (e.g., relative permeability, viscosity). This solution can be represented as a path in tie-line (Γ) space.

The second part deals with the hydrodynamic problem, which can be expressed using only two equations

$$\frac{\partial z_1}{\partial t} + \frac{\partial F_1}{\partial x} = 0, \qquad \ldots\ldots\ldots\ldots \quad (11)$$

$$\frac{\partial A_j z_1 + B_j}{\partial t} + \frac{\partial A_j F_1 + B_j}{\partial x} = 0. \qquad \ldots\ldots\ldots\ldots \quad (12)$$

for any fixed j. In these equations, the variation of γ in Γ-space is assumed to be a known function of a scalar parameter that varies monotonically along the path.

It can be shown that projection of stable waves and shocks, which form the solution of (8)-(9) for incompressible one-dimensional problems, into Γ-space corresponds to stable waves and shocks in the solution of the thermodynamic problem Entov (1997). Moreover, the solution path in Γ-space is independent of the hydrodynamic properties of the initial problem and depends only on the thermodynamic state (e.g., initial/injection compositions). Invariance of the solution path in Γ-space with respect to variation in the hydrodynamic variables was shown to be valid for compressible flows as

well (Voskov et al. (2001)).

Fig. 2 shows the projection of the solution, which is computed in standard compositional space, into Γ-space. In the figure, the solutions of three gas injection problems into oil made up of $\{CO_2, C_1, C_4, C_{10}\}$ are shown. The solutions are obtained for different space dimensions. The figure indicates that these solutions share (nearly) the same path in Γ-space.

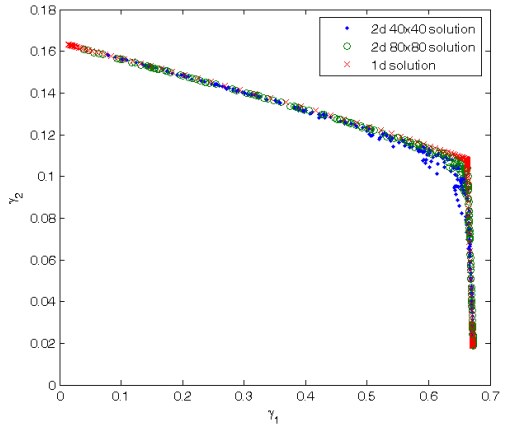

Fig. 2—Projection of solutions into Γ-space for 1D displacements (red) and 2D 5-spot displacements (blue for 40×40, green for 80×80) of oil made up of $\{CO_2, C_1, C_4, C_{10}\}$ by gas. All solutions are obtained using the Eclipse simulator.

It is difficult to say if solution invariance in Γ-space is a universal characteristic of all compositional problems. For a wide range of near-miscible gas injection problems with varying operating conditions, dimensionality, heterogeneity, and grid size, our computational experience indicates that the solutions are indeed nearly invariant in Γ-space.

In the next section, we show how this characteristic (i.e., the near invariance of the solution in tie-line space) can be used quite effectively to represent the phase behavior calculations associated with gas-injection problems in 1D. After that, we show that compositional space tabulation in terms of the tie-line parameterizations, both as a preprocessing step or with adaptive calculation, can be used to speed up the phase behavior calculations of standard compositional simulators for solving displacement problems of practical interest.

CSP-based Phase Behavior

We propose a new algorithm to replace the standard phase behavior approach, including phase-stability tests and flash calculations. Given the composition, pressure, and temperature, this procedure returns the liquid and vapor mole fractions , and the phase compositions. The approach makes use of the parameterized compositional space; as a result, we need to define x_1, y_1, A_i and B_i from (4) - (6) as a function of $\{p, T, \gamma\}$.

To simplify the description, we take the temperature T to be constant. For each pressure in the interval of interest, we construct the phase diagram and parameterize it using a finite number of tie-lines (Voskov (2002), Voskov et al. (2001)). All the parameterized tie-lines are stored in a table. For any given $\{p, z_i\}$, we solve the following optimization problem

$$\min_{\gamma} \left(\sum_{i=1}^{n_c} (A_i(\gamma) z_1 + B_i(\gamma) - z_i)^2 \right), \qquad \ldots\ldots\ldots\ldots \quad (13)$$

for phase diagrams j and $j+1$, where p^j and p^{j+1} are the endpoints of the interval under consideration. For both solutions γ^j, we calculate the respective x_i^j and y_i^j from (4) - (6). Then, using linear interpolation for pressure $p \in [p^j,\ p^{j+1}]$, we find x_i and y_i.

For example, Fig. 3 shows the tie-line that intersects the composition under study. The top and bottom diagrams are for pressures $p = 1470$ psi and $p = 1760$ psi, respectively. The absolute errors

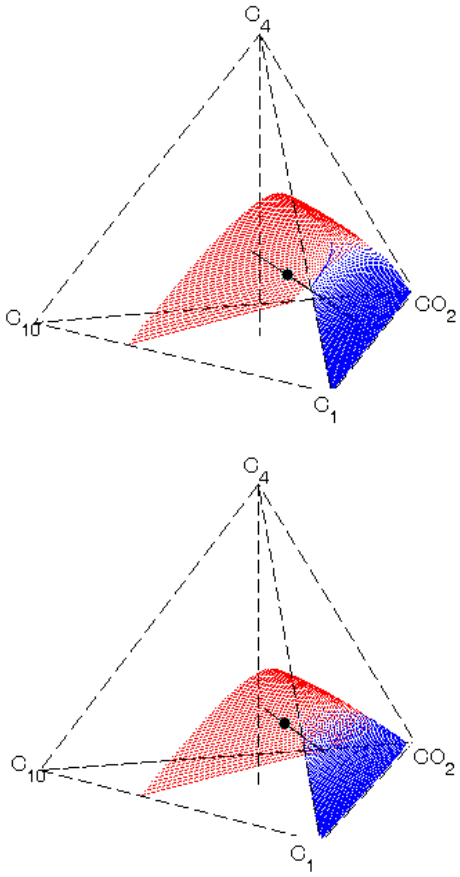

Fig. 3—Tetrahedral diagrams for a four-component $\{CO_2, C_1, C_4, C_{10}\}$ system at $p = 1470$ and $p = 1760$ psi ($T = 160^o$ F) and a randomly generated composition $\{0.31, 0.30, 0.21, 0.18\}$ with intersecting tie-lines.

in x_i and y_i obtained using the tie-line table look-up approach with pressure interpolation compared with standard EOS calculations are $\Delta x = 0.066\%$ and $\Delta y = 0.032\%$. Additional comparisons for several randomly chosen compositions and pressures are presented in Table 1 for the system $\{CO_2, C_1, C_4, C_{10}\}$, and in Table 2 for the system $\{N_2, C_1, C_3, C_6, C_{10}\}$. For each composition, flash calculations are performed for randomly chosen pressures in the interval $[1100, 2400]$ psi for the first table and $[1400, 2700]$ psi for the second table. The maximum difference for liquid and vapor fractions are shown in the tables. In order to obtain this precision level, several thousand tie-lines were collected for each pressure.

To demonstrate the CSP based table look-up approach, several numerical experiments were performed. Gas injection problems in one dimension were solved using a variety of injection and initial compositions. Here, we assume that the overall compressibility is low and that the dependence of composition on pressure differences is small.

First, we show the results for a problem where a gas composed of $\{CO_2(80\%), C_1(20\%)\}$ is injected into a homogeneous reservoir containing oil made up of $\{CO_2(5\%), C_1(20\%), C_4(30\%), C_{10}(45\%)\}$. For flash calculations, two tie-line based table look-up schemes were implemented. The first method take the closest tie-line from the table in order to minimize the norm of (13). These solutions are shown in Fig. 4 as green lines. In the second method,

Table 1–Flash computations 4-component system

Composition, %	Δx_{max},%	Δy_{max},%
{27, 22, 9, 42}	0.17	0.06
{28, 30, 19, 23}	0.23	0.08
{37, 42, 10, 11}	0.26	0.11
{39, 8, 7, 46}	0.1	0.03
{34, 52, 10, 4}	0.36	0.45
{38, 36, 18, 9}	0.27	0.26
{22, 37, 21, 20}	0.28	0.09
{46, 26, 19, 9}	0.23	0.11

Table 2—Flash computations 5-component system

Composition, %	Δx_{max},%	Δy_{max},%
{16, 32, 20, 8, 25}	0.13	0.16
{24, 33, 20, 14, 9}	0.24	0.21
{10, 36, 16, 29, 8}	0.59	0.19
{21, 11, 25, 25, 18}	0.08	0.12
{13, 24, 22, 18, 22}	0.12	0.31
{30, 16, 13, 16, 25}	0.14	0.15
{24, 29, 16, 26, 5}	0.11	0.16
{27, 12, 19, 3, 40}	0.15	0.27

Delaunay triangulation of the parameterized compositional space is performed, and the nonlinear problem (13) is solved for the interpolated functions. The solution using this method is shown in Fig. 4 as the red points. Simple Corey relative permeability curves and constant viscosities were used in the calculations. In Fig. 4, the two CSP-based solutions are compared with the standard compositional simulation results (blue line) obtained using Eclipse (2005). The small differences are due to ignoring the compressibility effects in the CSP-based simulations.

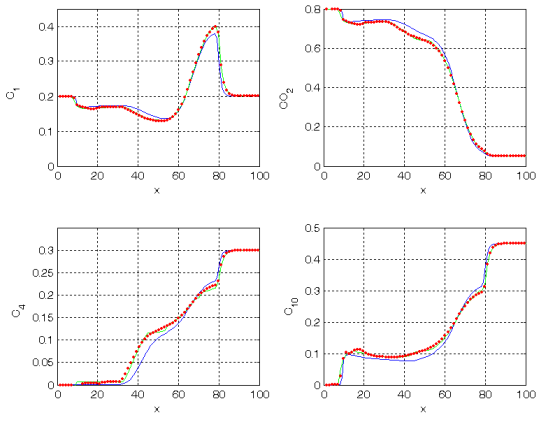

Fig. 4—Solution of gas injection problem into oil made up of $\{CO_2, C_1, C_4, C_{10}\}$. Red and green solutions - table look-up flash, blue - standard compositional solution.

Fig. 5 shows the results for a five-component gas-injection problem, where a gas composed of $\{N_2(85\%), C_1(10\%), C_3(3\%), C_6(1\%), C_{10}(1\%)\}$ is injected into a homogeneous medium to displace oil made up of $\{N_2(1\%), C_1(20\%), C_3(20\%), C_6(20\%), C_{10}(39\%)\}$.

The figure shows the solutions obtained from the two CSP-based methods (green and red lines) and standard simulation (blue line).

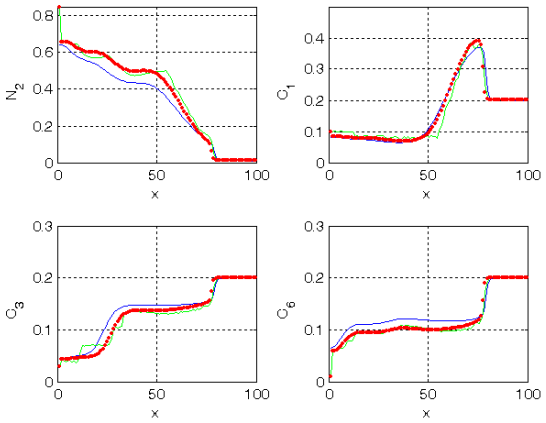

Fig. 5—Solution of gas injection problem into oil made up of $\{N_2, C_1, C_3, C_6, C_{10}\}$. Red and green solutions - table look-up flash, blue - standard compositional solution.

Compositional Space Tabulation

One can construct the tie-line parametrization as a pre-processing step. Then, the CSP approach described in the previous section can be used to replace standard EOS computations in flow simulation. In that case, however, a large number of tie-lines may be needed, and we have to contend with a high dimensional optimization problem (13). In this section, we modify the strategy so that we compute the necessary tie-lines only.

For gas injection processes, the solution route in compositional space can be split into two types: (1) tie-line paths, which connect points along a fixed tie-line (or its extension), and (2) non tie-line paths, where points on different tie-lines are connected (Orr (2007)). Thus, a limited number of key tie-lines are involved in the solution path. In practice, it is often the case that a single-phase gas mixture is injected to displace the resident hydrocarbon liquid. If the initial and injected compositions remain fixed during the displacement process and he pressure changes are small, the solution route involves these two tie-lines only (see Fig. 6).

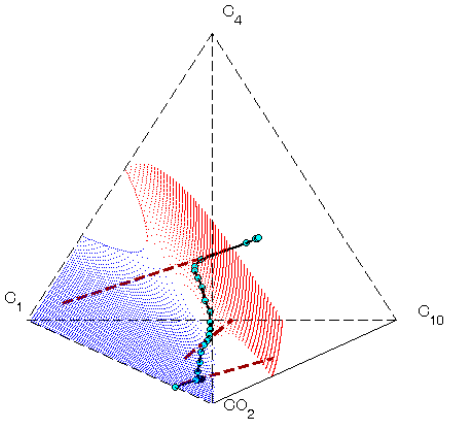

Fig. 6—Solution of gas injection problem for composition $\{CO_2, C_1, C_4, C_{10}\}$ in compositional space. In brown initial, injection and intermediate tie-lines are shown.

Compositional space tabulation (CST). For the particular displacement problem of interest, we specify a set of compositions and a pressure range. The composition set is chosen using information about the likely key tie-lines. The tie-lines associated with the initial and injection composition are obvious candidates. A table is constructed, where for each composition in the specified set, the tie-lines corresponding to each pressure value in the interval of interest are computed and stored.

During a flow simulation, whenever we need to perform a phase stability test, or run flash computations, we check if the composition lies on one of the stored tie-lines. To check the composition, we use a modification of (2)-(4)

$$L = \frac{z_j - y_j}{x_j - y_j} \quad \ldots\ldots\ldots\ldots\ldots (14)$$

$$\sum_{i=1}^{n_c} (x_i L + y_i(1-L) - z_i)^2 < \varepsilon. \quad \ldots\ldots\ldots\ldots\ldots (15)$$

If one of the stored tie-lines satisfies these criteria for the composition of interest, the table is used to look up the flash results. Otherwise, a standard EOS based phase behavior procedure is employed. In this procedure, which we refer to as Compositional Space Tabulation (CST), we work with the precomputed table of tie-lines, and any composition, which does not intersect one of the tie-lines in the table, is handled using a standard EOS scheme.

Compositional Space Adaptive Tabulation (CSAT). For compositions that lie on one of the tie-lines in the table, the CST method replaces all phase behavior calculations. In compositional simulation practice, however, the phase stability test is the most time consuming procedure. The number of iterations to perform the phase stability tests is usually very large (see Table 3), and each iteration takes a significant number of arithmetic operations.

In order to speed up the phase stability test, we propose a Compositional Space Adaptive Tabulation (CSAT) strategy. Each time a phase-state stability test is required during a compositional simulation, we check the set of stored tie-lines. If the composition does not lie on any of the stored tie-lines, new tie-lines are computed for the pressure range of interest. The CSAT method was implemented in a General Purpose Research Simulator (GPRS) Cao (2002).

In addition to the phase stability test, the CSAT method can be used to replace standard flash calculations. In that case, a more sophisticated algorithm for tie-line checking (14)-(15) is needed because the number of tie-lines can be quite large.

Tie-line calculation procedure. The CST and CSAT schemes require the computation of a tie-line for any composition and pressure interval. For compositions in the two-phase region, a tie-line is computed using standard EOS based flash calculations. For compositions in the single-phase state, but within the region of tie-line extensions, a procedure to calculate the tie-line extension is needed. A negative flash calculation can be used for that purpose (see Whitson and Michelsen (1989)). Here associated with negative flash calculations, we present a different algorithm to calculate tie-line extensions:

1. Find the longest tie-line in compositional space.
2. Connect the composition with a bubble, or dew, point for this tie-line. This is dictated by the original state of the composition. For liquid, we connect with a dew point, and for vapor, we connect with a bubble point.
3. Traverse the tie-line from the initial single-phase composition, and find the first point inside the two-phase region.
4. For the located point, perform flash calculations, and find the new tie-line.
5. Repeat the procedure starting from the second step until convergence.

For the pressure value of interest, this algorithm shows good convergence properties for compositions located in the region of tie-line extensions.

For cases with super-critical compositions, a modification of the tie-line calculation procedure is necessary.

Tests for Adaptive Tabulation Method

In this section we are going to present different tests for immiscible Compositional Space Adaptive tabulation. We are going to investigate the general distribution of the tie-lines in compositional space for simple four-component system as well as present the performance results for the reservoir simulation cases.

Tie-Lines Distribution for CSAT. The test cases are built based on the four-component system $\{CO_2, C_1, C_4, C_{10}\}$. A gas mixture $\{CO_2\ (90\%), C_1\ (10\%)\}$ is injected into oil composed of $\{CO_2(1\%), C_1(20\%), C_4(29\%), C_{10}(50\%)\}$. Here we choose the four component system in order to present the CSAT results on a compositional diagram. Three homogeneous cases are presented:

- A one dimensional (300 cells) problem with injection and production wells in the first and last grid blocks, respectively
- A three dimensional $(10 \times 10 \times 3)$ problem with injection and production wells at the corners
- A three dimensional $(40 \times 40 \times 12)$ problem $(4 \times 4 \times 4$ refinement) with injection and production wells at the corners

For all three tests, injection and production wells operate at Bottom Hole Pressure control of $p = 1500$ and $p = 500$ psi, respectively. These pressures define the interval used for CSAT parameterization.

Fig. 7 shows the solution of the one-dimensional problem in compositional space. For this case, CSAT collects 12 tie-lines during the simulation. The first (injection) and the last (production) tie-lines are labeled with bold end-points on the diagram. These two tie-lines are used in more than 98% of all phase stability checks. The rest of the tie-lines are used in the construction of the solution during the early period, when all shocks and rarefractions have not evolved fully.

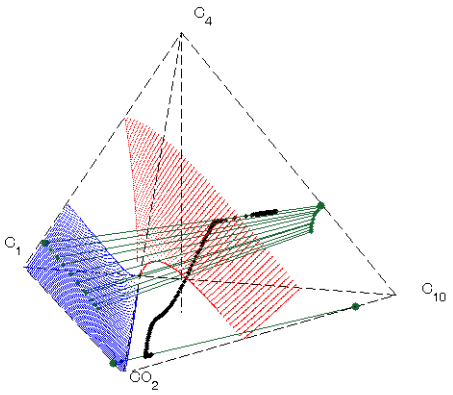

Fig. 7—(a) 1D gas injection solution. Corresponding CSAT tie-lines. Blue and red are dew and bubble points respectively for $p = 1100$ psi.

The next test is a 3D modification of this case. The number of tie-lines collected by CSAT remains the same, but in this case intermediate tie-lines (different from the injection and initial tie-lines) are more involved in the phase stability checks. From Fig. 8(a), one can see that the location of these tie-lines is very similar to the 1D case. Fig. 8(b) shows the number of checks for each tie-line at a given time. Here T is a gas breakthrough time for the model.

The last test from this set is the refined 3D model. The displacement path from the refined model is less dispersive, as shown in Fig. 9 (a); however, as indicated by Fig. 9 (b) the tie-line profile used by CSAT is largely unchanged. Only a few additional tie-lines are needed near the end of the displacement process, and they are

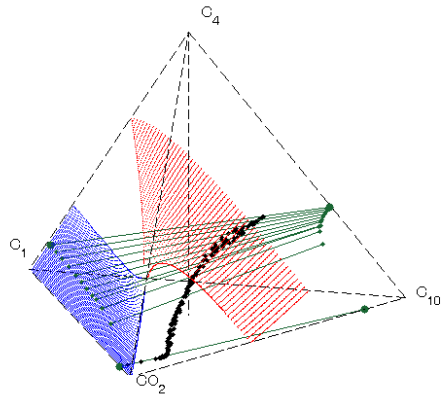

(a)

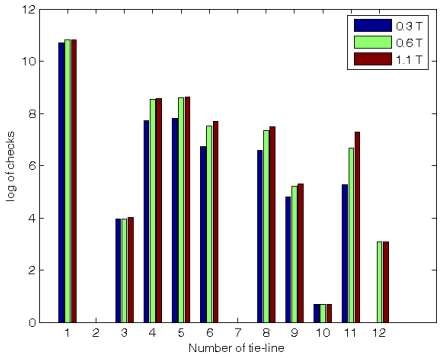

(b)

Fig. 8—(a) Solution of 3D problem in compositional space with corresponding CSAT tie-lines, and (b) diagram for successful CSAT tie-line checks at different times of simulation. Blue and red are dew and bubble points respectively for $p = 1100$ psi.

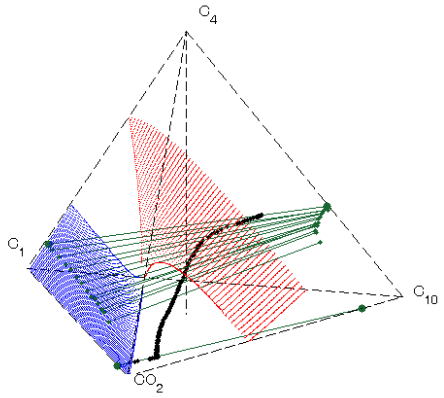

(a)

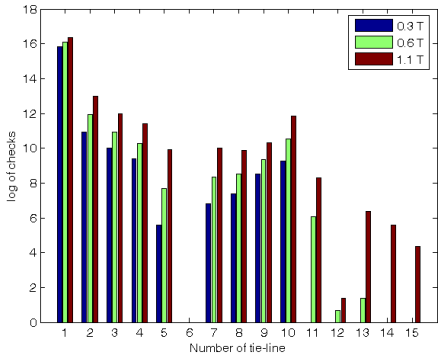

(b)

Fig. 9—(a) Solution of 3D problem in compositional space with corresponding CSAT tie-lines, and (b) diagram for successful CSAT tie-line checks at different times of simulation. Blue and red are dew and bubble points respectively for $p = 1100$ psi.

associated with breakthrough of compositions located around the leading shocks.

The next simulation set is built from the fluid description of the SPE 3 problem. The original SPE 3 case is an immiscible depletion problem, where the initial composition is very close to the dew-point. The oil is composed of nine components $\{CO_2$ (1.2%), N_2 (1.9%), C_1 (16%), C_2 (8.7%), C_3 (5.9%), C_{4-6} (9.7%), C_{7+1} (4.7%), C_{7+2} (11.5%), C_{7+3} (40.3%)$\}$. We added a well that injects a mixture of gases ($\{N_2$ (90%), C_1 (10%)$\}$ at immiscible downhole conditions. Again we vary the model using three homogeneous configurations:

- A one dimensional (500 cells) problem with injection and production wells in the first and last grid blocks, respectively
- A three dimensional ($10 \times 10 \times 5$) problem with injection and production wells at the opposite corners

For both tests, injection and production wells operate using Bottom Hole Pressure control at $p = 2000$ and $p = 500$ psi, respectively.

Fig. 10(a) distribution of successful tie-line checks for one-dimensional gas injection problem at different times. Again only the initial (first) and injection (seventh) tie-lines are involved in CSAT checks. The rest of the tie-lines are involved in the solution only during the early stages.

Fig. 10(b) shows a diagram of the tie-line distribution for 3D model at different times. As for four component case, CSAT uses a limited number of tie-lines, and the refined model leads to a few additional tie-lines during the late stages of the displacement.

Description of test cases. To demonstrate the CST and CSAT approaches, we consider several test cases:

- Case 1: Injection of C_1 into oil made up of $\{C_1$ (4%), C_4 (16%), C_{7+1} (20%), C_{7+2} (60%)$\}$. A sector of a 5-spot pattern, discretized using $10 \times 10 \times 5$ gridblocks, with an injector (at 600 psi) and a producer (at 400 psi) in the corners.
- Case 2: Injection of a gas mixture composed of $\{N_2$ (80%),C_1 (10%),$C2$ (10%)$\}$ into oil made up of $\{CO_2$ (1.2%), N_2 (1.9%), C_1 (16%), C_2 (8.7%), C_3 (5.9%), C_{4-6} (9.7%), C_{7+1} (4.7%), C_{7+2} (11.5%), C_{7+3} (40.3%)$\}$. A 5-spot pattern, discretized using $10 \times 10 \times 5$ gridblocks, is used. An injection well, operating at 2000 psi, is placed in the center, and four production wells, each operating at 1000 psi, are at the corners. The thermodynamic properties are (mostly) taken from the SPE 3 comparative solution problem.
- Case 3: Same as Case 2, but with $20 \times 20 \times 5$ gridblocks.
- Case 4: Same as Case 2, but with $50 \times 50 \times 5$ gridblocks.
- Case 5: Same model as in Case 2, but with different initial and injection compositions. The injection composition is $\{N_2$ (90%), C_1 (10%)$\}$ and the initial oil composition is $\{CO_2$ (1.2%), N_2 (1.9%), C_1 (26%), C_2 (8.7%), C_3 (5.9%), C_{4-6} (9.7%), C_{7+1} (4.7%), C_{7+2} (11.5%), C_{7+3} (30.3%)$\}$.
- Case 6: C_1 injection into oil made up of $\{C_1$ (30%), C_3 (3%), C_6 (7%), C_{10} (20%), C_{15} (40%)$\}$. It is a 5-spot $10 \times 10 \times 5$ sector with a production well (at 1000 psi) and an injection well (at 3000 psi) in the corners. This case is similar to the SPE 5 problem.
- Case 7: Same as Case 6, but with $500 \times 1 \times 1$ gridblocks. The injector and producer are in the first and last gridblocks, respectively.

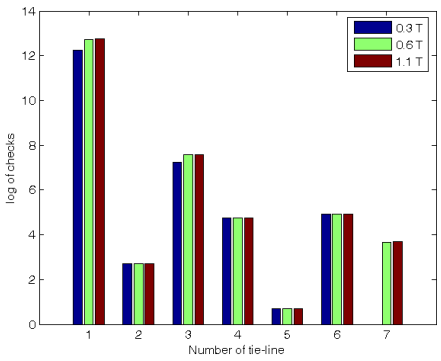

(a)

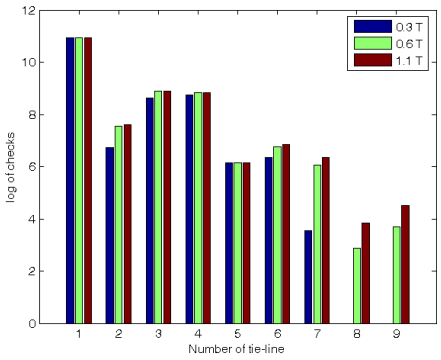

(b)

Fig. 10—SPE 3 diagram for successful CSAT tie-line checks for 1D (a) and 3D (b) gas injection cases.

- Case 8: The SPE 5 WAG injection problem. The reservoir model is made up of $7 \times 7 \times 3$ gridblocks. Gas is composed of $\{C_1$ (77%), C_3 (20%), C_6 (3%)$\}$. The oil composition is $\{C_1$ (50%), C_3 (3%), C_6 (7%), C_{10} (20%), C_{15} (15%)$\}$, C_{20} (5%)$\}$. Water and gas are injected in one corner at 5000 psi, the production well is in the opposite corner operating at 3000 psi. The injected gas is miscible with the resident oil for the pressure interval of interest that makes this case multi-contact miscible.
- Case 9: Same as Case 8 but instead of WAG we inject only gas with the same composition.

Computational Results. Table 3 presents results obtained using CST, CSAT and standard EOS methods for the eight test cases. In the CST method, only the injection and initial compositions were used for the phase stability test. The CSAT scheme was used with different values for the tolerance ε. The stability iteration count reported in the table includes phase-stability tests for both reservoir and surface conditions. Table 3 also shows the number of tie-line checks (see CSAT description) performed. The EOS time includes the time spent on stability tests, flash calculations, and tie-line checking (both tie-line look-up and computation of new tie-lines as needed by CSAT). In most cases, SSI is the fastest option for small problems when the displacement takes place in the region that can be represented by tie-lines. However, in many instances, SSI should be supplemented by Newton iterations. Cases 2, 3, 8 and 9 were run using an SSI-Newton combination. For these cases, the SSI and Newton iterations are reported, respectively, in the stability iteration column.

As indicated in Table 3, the CSAT method with $\varepsilon = 10^{-3}$ for Cases 7 and 8 uses one tie-line only. This is because the injection and production tie-lines turn out to be very close to each other. At first glance, this may seem surprising. However, note that gas is injected at 3000 psi. For this fluid system, the two-phase region at this high pressure is quite small, and most of the tie-lines are close to each-other. In Case 8, for the pressure interval under study, the injection gas is miscible with the resident oil. For this case, only one (the initial) tie-line was used in the CST procedure.

Table 4 shows the dependance of the CSAT method on the number of pressure intervals in the tie-line table. A study of Table 4 shows that the number of computed tie-lines depends only slightly on the number of pressure intervals used. These results demonstrate that tie-lines vary almost linearly even when the pressure variations are significant.

Table 5 shows two miscible cases with injection composition in the super-critical (i.e., beyond tie-line extensions) region. The effect of the number of pressure points, *n*, used in the tie-line table is also reported, namely, n = 5 and 10. Analysis of the results in the Table 5 indicates that the CSAT method is not very effective when one of the compositions is in the super-critical (i.e., beyond tie-line extensions) region. Significant improvement are obtained, however, when information about the applicable MMP is used in the tie-line table. We note that for tie-line interpolation in the neighborhood of the super-critical region, the use of more pressure points, or a more sophisticated interpolation scheme, may be beneficial.

Fig. 11 presents the projection of solutions in Γ-space for two five-component gas injection problems (cases 6 and 7). Green points show projection of the 1D solutions, blue points represent the 3D solutions. The red x's show the tie-lines for $\varepsilon = 10^{-5}$, and the black o's represent tie-lines with a tolerance $\varepsilon = 10^{-6}$. Notice that most of the tie-lines in the table are concentrated around the initial tie-line (beginning of the path in Γ-space).

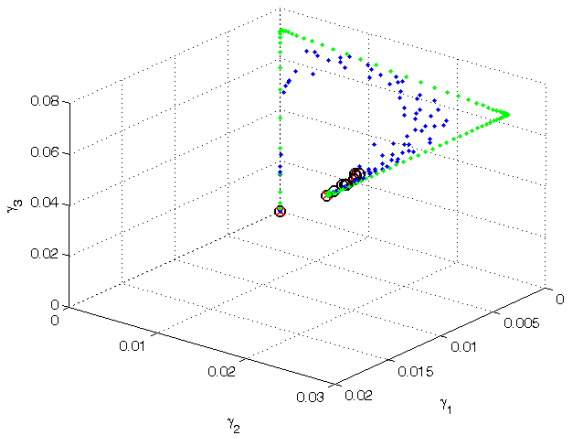

Fig. 11—Projection of solutions of cases 6 and 7 into Γ-space. Green points show projection of the 1D solutions, blue points show projection of the 3D solution. Red x and black o symbols show projection of CSAT tie-lines for $\varepsilon = 10^{-5}$ and $\varepsilon = 10^{-6}$, respectively.

The compositional space in the region beyond tie-line extensions (super-critical region) cannot be represented using the Γ-space. So, if the solution path in the course of a simulation crosses the region of tie-line extensions, we resort to standard EOS computations. We are looking into ways to complement the tie-line parametrization in the region of tie-line extensions with an effective representation of the super-critical compositional space.

Conclusions

We presented a multi-component, multi-phase, reservoir flow simulation methodology based on the parametrization of the compositional space using tie-lines. CST can be used to replace all phase behavior calculations (i.e., phase stability and flash). The adaptive tabulation scheme, CSAT, can be used most effectively to replace the phase stability test in conventional EOS compositional simula-

tors. CST and CSAT were implemented in a General Purpose Research Simulator (GPRS). Using a variety of challenging compositional gas-injection problems, we show that compared to standard approaches, CSAT leads to very large improvements (at least an order of magnitude) in the performance of phase behavior computations. We note that these tie-line based parametrization schemes can be incorporated into existing simulations relatively easily.

The remaining major challenge is the fact that beyond the region of tie-line extensions (i.e., super-critical region), tie-lines are not defined, and thus by definition a tie-line based parametrization of that region is not possible. We have an ongoing research effort to develop an effective representations of the phase behavior in the super-critical region in a manner that complements the tie-line based parametrization framework described here.

Nomenclature

p	Pressure
T	Temperature
z_i	overall mole fractions of component *i*
x_i	oil mole fractions
y_i	gas mole fractions
L	liquid phase volumetric fraction
$f_{i,V}$	fugacity of component *i* in vapor phase
$f_{i,L}$	fugacity of component *i* in liquid phase
A_i	parameters for tie-line representation
B_i	parameters for tie-line representation
γ	tie-line parameter
F_i	fractional flow of component *i*
$F(s)$	fractional flow of the liquid phase
U	total velocity
m	porosity of reservoir
ε	tolerance for tabulation

Acknowledgements

We thank Chevron, Schlumberger and Total companies as well as SUPRI-B Industrial Affiliates' program for financial support.

References

Coats K.H., An Equation of State Compostional Model. - SPEJ, 1980, v.20, N 5.

Nghiem L.X., Fong D.K., Aziz K., Compositional Modeling With an Equation of State. - SPEJ, 1981, vol.21, N 6.

Chien M.C.H., Lee S.T., Chen W.H., A New Fully Implicit Compositional Simulator. - SPE 13385, 1985.

Aziz, K. and Wong, T.W., ŞConsiderations in the Development of Multipurpose Reservoir Simulation ModelsŤ, proceedings of the 1st and 2nd International Forum on Reservoir Simulation, Alpbach, Austria, September 12-16, 1988 and September 4-8, 1989.

Helfferich F.G. Theory of multicomponent, multiphase displacement in porous media. - SPEJ, 1981, v.21, N 1, p.51-62.

Barenblatt G.I., Entov V.M., Ryzhik V.M. Fluids Flow through Natural Rocks, Dordrecht, Kluwer, 1990

Brusilovsky A.I., Zazovsky A.F., A new approach to modeling of multi-component two-phase EOR processes with interphase mass exchange. SPE 22638, 1991.

Tang D.E., Zick A.A., A new limited compositional reservoir simulator. SPE 25255, 1993

Monroe, W.W., Silva, M.K., Larsen, L.L., Orr, F.M.Jr., Composition paths in four-component systems: effect of dissolved methane on 1D CO_2 flood performance, Soc.Petr.Eng. Res.Eng. 1990, 5, 423-432.

Johns, R.T., Dindoruk B., Orr F.M. Jr., Development of miscibility in four-component CO_2 floods, Soc.Petr.Eng. Res.Eng. 1993, 8, 135-142.

Johns R.T., Dindoruk B., Orr F.M. Jr., Analytical theory of combined condensing/vaporising gas drives. Soc. Petr. Engrs. Advanced Technology Series, 1993, 1(2), 7-16.

Franklin M. Orr, Jr., Theory of Gas Injection Processes, Tie-Line Publications, Copenhagen, 2007.

Entov V.M., Nonlinear waves in physicochemical hydrodynamics of enhanced oil recovery. Multicomponent flows, Proc. of the International Conference "Porous Media: Physics, Models, Simulations," Moscow, 19-21 Nov., 1997, A.Dmitrievsky, M.Panfilov, eds., World Scientific, Singapore, 1999, pp.33-56.

Entov V.M., Voskov D.V., On oil displacement by gas injection: constant partition coefficients case, in: Proc. International Conf. "Modern Approaches to Flows through Porous Media", Moscow, Sept.6-8, 1999, II-32-II-34.

Entov V.M., Voskov D.V., On oil displacement by gas injection, Proc.;, 7th European Conference on the Mathematics of Oil Recovery, Baveno, Italy, 5-8 Sept., 2000.

Entov V.M., Voskov D.V., On oil displacement by gas injection, *Izv. Ross. AN, Mekh. Zhidk. i Gaza*, 2001, N2.

Voskov D.V., Entov V.M., Turetskaya F.D., On approximation of phase equilibria of multicomponent hydrocarbon mixtures and prediction of oil displacement by gas injection. Proc.; 8th European Conference on the Mathematics of Oil Recovery, Freiburg, Germany, 4-7 Sept., 2001.

Voskov D.V., Two-Phase Multicomponent Flows through Porous Media, PhD Thesis, 2002, Gubkin Russian State Oil and Gas U., Moscow, Russia.

Bedrikovetsky P.G., Chumak M.L., Riemann problem for two–phase four- and more component displacement (gas processes). 1992, Proc of 3rd European Conference on the Mathematics of Oil Recovery. Delft, The Netherlands.

Michelsen, M.L., "Speeding up the two-phase PT-flash, with application for calculation of miscible displacement", Fluid Phase Equilibria, vol: 143, pages: 1-12, 1998.

Firoozabadi A, Pan H. Fast and robust algorithm for the compositional modeling: Part I. Stability analysis testing. SPE J. 2002; March:78-89.

Rasmussen C.P., Krejbjerg K., Michelsen M.L., Bjurstrom K.E.: Increaseng of computational speed of flash calculations with applications for compositional, transient simulations, SPE REE, February, 2006

Michelsen M.L., The isothermal flash problem: Part I. Stability. Fluid Phase Equilibria, 9: 1-19, 1982.

Michelsen, M.L. and Mollerup, J.M., Thermodynamic Models: Fundamentals and Computational Aspects, Tie-Line Press, Holte, Denmark (2004).

Eclipse Technical Description, Schlumberger, 2005

Cao H., Development of Techniques for General Purpose Simulators, Ph.D. Thesis, Stanford University, 2002

Whitson, C.H. and Michelsen, M.L., The Negative Flash, Fluid Phase Equilibria 53 (1989), 51Ű71.

Denis V. Voskov is a Senior Research Associate in the Department of Energy Resources Engineering at Stanford University. e-mail: dvoskov@stanford.edu **Hamdi A. Tchelepi** is Associate Professor of Energy Resources Engineering at Stanford University. e-mail:tchelepi@stanford.edu.

Table 3: Comparison between standard, CST, and CSAT compositional simulation methods for eight study cases

Test case	Type of EOS calc.	Stab. it., 10^3	Check it.,10^3	Tie-lines	EOS time, sec
Case 1	original	3012	–	–	29
	CST	5	222	2	< 1
	CSAT ($\varepsilon = 10^{-4}$)	4	223	5	< 1
	CSAT ($\varepsilon = 10^{-5}$)	4	233	14	< 1
Case 2	original	1442 + 366	–	–	27
	CST	174 + 489	205	2	4
	CSAT ($\varepsilon = 10^{-3}$)	23 + 7	216	9	< 1
	CSAT ($\varepsilon = 10^{-4}$)	15 + 5	286	25	1
Case 3	original	7459 + 1671	–	–	144
	CST	1204 + 290	978	2	25
	CSAT ($\varepsilon = 10^{-3}$)	37 + 11	1254	12	4
	CSAT ($\varepsilon = 10^{-4}$)	26 + 8	1983	60	6
Case 4	original	95071 + 19873	–	–	1674
	CST	15620 + 3678	11762	2	323
	CSAT ($\varepsilon = 10^{-3}$)	134 + 38	14806	19	52
	CSAT ($\varepsilon = 10^{-4}$)	77 + 23	28463	101	50
Case 5	original	921	–	–	7
	CST	62	106	2	1
	CSAT ($\varepsilon = 10^{-3}$)	28	120	8	< 1
	CSAT ($\varepsilon = 10^{-4}$)	19	142	28	2
Case 6	original	9309	–	–	35
	CST	41	404	2	< 1
	CSAT ($\varepsilon = 10^{-3}$)	9	398	1	< 1
	CSAT ($\varepsilon = 10^{-4}$)	8	402	2	< 1
	CSAT ($\varepsilon = 10^{-5}$)	8	409	4	< 1
	CSAT ($\varepsilon = 10^{-6}$)	8	440	10	< 1
Case 7	original	12821	–	–	54
	CST	20	936	2	< 1
	CSAT ($\varepsilon = 10^{-3}$)	20	928	1	< 1
	CSAT ($\varepsilon = 10^{-4}$)	18	936	2	< 1
	CSAT ($\varepsilon = 10^{-5}$)	18	936	4	< 1
	CSAT ($\varepsilon = 10^{-6}$)	18	937	9	< 1
Case 8	original	15001+1490	–	–	101
	CST	7956+581	227	1	52
	CSAT ($\varepsilon = 10^{-3}$)	4678+206	448	3	39
	CSAT ($\varepsilon = 10^{-4}$)	5320+271	723	7	68

Table 4: Effect of the number of values used to represent the pressure range in CSAT simulations

Test case	N pressures	Stab. it., 10^3	Check it.,10^3	Tie-lines	EOS time, sec
Case 2	2	17 + 5	263	22	0.6
CSAT ($\varepsilon = 10^{-4}$)	3	16 + 5	282	25	0.7
	5	15 + 5	286	25	1.2
	10	15 + 5	287	24	2.2
	20	15 + 5	287	26	3.9

continued on next page

continued from previous page					
Test case	N pressures	Stab. it., 10^3	Check it.,10^3	Tie-lines	EOS time, sec
Case 3	2	29 + 9	1842	64	5.4
CSAT ($\varepsilon = 10^{-4}$)	3	26 + 8	1979	59	5.6
	5	26 + 8	1983	60	7.4
	10	25 + 7	1964	62	8.3
	20	25 + 7	1965	62	10.5
Case 4	2	247 + 70	13873	18	48.5
CSAT ($\varepsilon = 10^{-3}$)	5	134 + 38	14806	19	52.2
	20	132 + 38	14843	19	47.9
Case 4	2	100 + 29	28316	105	50.4
CSAT ($\varepsilon = 10^{-4}$)	5	77 + 23	28463	101	50.3
	20	77 + 23	28413	102	57.3
Case 6	2	17	408	4	0.9
CSAT ($\varepsilon = 10^{-5}$)	3	11	409	4	0.8
	5	10	409	4	1.0
	10	8	409	4	0.6

Table 5: Comparison of standard and various CSAT schemes for super-critical miscible simulations

Test case	Type of EOS calc.	Stab. it., 10^3	Check it.,10^3	Tie-lines	EOS time, sec
Case 8	original	15001+1490	–	–	101
($\varepsilon = 10^{-3}$)	CSAT, $n = 5$	4678+206	448	3	39
	CSAT (corr.), $n = 5$	2242+73	877	7	18
	CSAT (corr.), $n = 10$	1891+58	894	7	18
Case 9	original	8171+1022	–	–	58
($\varepsilon = 10^{-3}$)	CSAT, $n = 5$	4050+252	247	3	51
	CSAT (corr.), $n = 5$	1860+102	800	7	21
	CSAT (corr.), $n = 10$	733+40	829	7	14